Sliding Mode Control with Fixed Switching Frequency for Four-Wire Shunt Active Filter

Farid Hamoudi*, A.Aziz Chaghi**, Hocine Amimeur**, El Kheir Merabet**

*Electrical and Electronic Engineering Institute, Boumerdès University,
Independence Avenue, Boumerdès 35000, Algeria.
Tel-Fax: +213 248 183 33, E-mail: f_hamoudi@yahoo.fr.
**LSPIE Laboratory, Electrical Engineering Department, Batna University,
Street Md El Hadi Boukhlouf, Batna 05000, Algeria.

***Abstract*—The present paper proposes a sliding mode control with fixed switching frequency for three-phase three-leg voltage source inverter based four-wire shunt active power filter, to improve phase current waveform, neutral current mitigation and reactive power compensation in electric power distribution system. The performed sliding mode for active filter current control is formulated using elementary differential geometry, and the discrete control vector is deduced from the sliding surface accessibility using the Lyapunov stability. The problematic of the switching frequency has been treated considering hysteresis comparators for the switched signals generating. In this way, a variable hysteresis band has been established as a function of the sliding mode equivalent control and a predefined switching frequency in order to keep this one always constant. The proposed control has been verified with computer simulation which showed satisfactory results for the above objectives.**

***Index Terms*—Sliding mode control, Switching frequency, Four-wire active filter, current harmonics compensation.**

I. Introduction

The three-phase four-wire active power filters are nowadays attracting more interest for researchers in power quality conditioning [1]- [9]. Two configurations of voltage source inverter (VSI) can be used to implement three-phase four-wire active filters, the first one use a fourth leg to provide the neutral current, where the second configuration uses a conventional three-leg converter with two cascade connected capacitors in the DC-bus and the neutral wire is connected directly to the midpoint of this bus. Although the four-leg configuration is preferable for its simple controllability [5] [10], the three-leg configuration which used in this paper is preferable for its reduced number of semi-conductors.

The computation of compensated components is the first required step in active filter control, it is used to identify the undesirable component to be suppressed and eventually some additional component needed to compensate the active filter losses. Several control algorithms, such as instantaneous reactive power theory [11], synchronous reference frame [7], and fast Fourier transform method [12] are used in this way. The VSI is then forced to inject these components in the point of common coupling with minimum error and fast response. This objective requires an appropriate current control method. In this way, the sliding mode control (SMC) which is derived from the theory of variable structure control, known as a discontinuous control technique taking in account the time varying topology of the controlled system is naturally suitable to control systems based on power electronics devices in general [13]- [18], and active filter as particular case of these systems [19]- [21]. It is characterized by simplicity implementation, fast response and high robustness. However, the ideal sliding motions imply infinite frequency in the switched signals which is naturally impossible to achieve in practice, where the switching frequency must be not only finite but also stable. The idea of fixed frequency control in power converters has been treated in several works [22]- [28]. Most of these contributions are based on the relation between the switching frequency and the average control also called equivalent control and it has been shown that it is possible to modulate this continuous control to generate the switched signals with fixed frequency, by using PWM modulation [23] [29] or $\Sigma - \Delta$-modulation [18].

The present paper proposes to generate the switching signals through hysteresis comparators, this one is very popular in current control application, and it is often used in sliding mode implementation in order to limit the switching frequency. Although simple and extremely robust [30], the switching frequency remains free and varies considerably with respect to the state variables when the hysteresis bandwidth is fixed preliminary. However, it has been shown in several works [22] [24]- [27] [30] that it is possible to keep this frequency constant with adopting a variable hysteresis bandwidth. The idea developed in this work consists to implement the sliding mode control with varying the hysteresis bandwidth instead of the switching frequency which is needed to be constant. This paper is presented as follows: after this introduction, a brief description and modeling of the active filter are presented in section II, after that, the principe of the compensated components computation is presented section III. The aim object of the paper is treated in detail in section IV, and the computer simulations are given in section V. Finally the paper is ended by a conclusion.

II. System Description and Modeling

Figure. 1 illustrates the basic compensation principle of the four-wire shunt active power filter (SAPF). The power circuit is based on three-phase three-leg controlled current voltage source PWM inverter connected to the grid at the AC

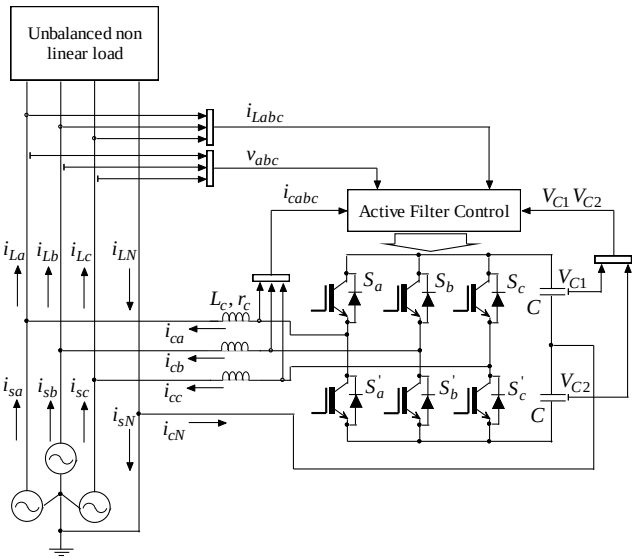

Fig. 1. Three-phase three-leg VSI based four-wire shunt active filter.

side through a passive filter (L_c, r_c) and uses two cascade connected capacitors $C_1 = C_2 = C$ as voltage source at the DC side, with the midpoint connected to the neutral wire of the grid to compensate neutral load current. An unbalanced nonlinear load is considered as a polluting source that draws unbalanced and distorted currents i_{Labc} from the mains. The SAPF is controlled to inject compensated current vector i_{cabc} in the grid in order to achieve source currents i_{sabc} balanced, sinusoidal and in phase with the fundamental main voltages, with keeping the DC-link voltages V_{C1} and V_{C2} balanced and in an admissible range. To establish the dynamic equations of the system, let suppose that the power switches S_j can be assumed ideals, then the output voltage for each phase j to neutral can be expressed as follows:

$$v_{cj} = d_j V_{C1} - \bar{d}_j V_{C2} \tag{1}$$

$d_j (j = a, b, c)$ are the PWM switching functions given by:

$$d_j = \frac{u_j + 1}{2} \tag{2}$$

Where u_j is associated to the power switch states as follows:

$$\begin{aligned} u_j = 1 \quad & \text{If } S_j \text{ on and } S'_j \text{ off} \\ u_j = -1 \quad & \text{If } S_j \text{ off and } S'_j \text{ on} \end{aligned}$$

Replacing (2) in (1) the active filter voltage is then rewritten as follows:

$$v_{cj} = \frac{1}{2} u_j (V_{C1} + V_{C2}) + \frac{1}{2}(V_{C1} - V_{C2}) \tag{3}$$

The DC-bus voltages across the two capacitors are related to u_j and the active filter currents i_{cj} as follows:

$$\frac{dV_{C1}}{dt} = \frac{1}{2C}\Big(\sum_{j=a,b,c} u_j i_{cj} + \sum_{j=a,b,c} i_{cj} \Big) \tag{4}$$

$$\frac{dV_{C2}}{dt} = \frac{1}{2C}\Big(\sum_{j=a,b,c} u_j i_{cj} - \sum_{j=a,b,c} i_{cj} \Big) \tag{5}$$

From the Kirchhoff's voltage law, the interaction between the voltage source inverter and the grid is described by following differential equation:

$$L_c \frac{di_{cj}}{dt} = -r_c i_{cj} + \frac{1}{2} u_j V_{dc} + \frac{1}{2}(V_{C1} - V_{C2}) - v_j \tag{6}$$

Where v_j represent the main voltages at the point of common coupling. Finally, these equations are rearranged under matrix from:

$$\dot{\boldsymbol{x}} = \boldsymbol{A}\boldsymbol{x} + \boldsymbol{B}(\boldsymbol{x})\boldsymbol{u} + \boldsymbol{v} \tag{7}$$

Where:

$$\boldsymbol{x} = \begin{bmatrix} i_{ca} & i_{cb} & i_{cc} & V_{C1} & V_{C2} \end{bmatrix}^T$$

$$\boldsymbol{A} = \begin{bmatrix} -\frac{r_c}{L_c} & 0 & 0 & \frac{1}{2L_c} & -\frac{1}{2L_c} \\ 0 & -\frac{r_c}{L_c} & 0 & \frac{1}{2L_c} & -\frac{1}{2L_c} \\ 0 & 0 & -\frac{r_c}{L_c} & \frac{1}{2L_c} & -\frac{1}{2L_c} \\ \frac{1}{2C} & \frac{1}{2C} & \frac{1}{2C} & 0 & 0 \\ -\frac{1}{2C} & -\frac{1}{2C} & -\frac{1}{2C} & 0 & 0 \end{bmatrix}$$

$$\boldsymbol{B}(\boldsymbol{x}) = \begin{bmatrix} \frac{V_{dc}}{2L_c} & 0 & 0 \\ 0 & \frac{V_{dc}}{2L_c} & 0 \\ 0 & 0 & \frac{V_{dc}}{2L_c} \\ \frac{i_{ca}}{2C} & \frac{i_{cb}}{2C} & \frac{i_{cc}}{2C} \\ \frac{i_{ca}}{2C} & \frac{i_{cb}}{2C} & \frac{i_{cc}}{2C} \end{bmatrix}$$

$$\boldsymbol{u} = \begin{bmatrix} u_a & u_b & u_c \end{bmatrix}^T, \ \boldsymbol{v} = \begin{bmatrix} -\frac{v_a}{L_c} & -\frac{v_b}{L_c} & -\frac{v_c}{L_c} & 0 & 0 \end{bmatrix}^T$$

III. Principe of Operation

In four-wire systems the current drawn by an unbalanced nonlinear load contains positive-sequence, negative-sequence and zero-sequence harmonic components that can be expressed in $\alpha\beta\gamma-$frames and arranged in matrix form as follows:

$$\boldsymbol{i}_{L\alpha} = \begin{bmatrix} i^+_{L\alpha 1} & i^+_{L\alpha 2} & \dots & i^+_{L\alpha n} & i^-_{L\alpha 1} & i^-_{L\alpha 2} & \dots & i^-_{L\alpha n} \end{bmatrix}$$

$$\boldsymbol{i}_{L\beta} = \begin{bmatrix} i^+_{L\beta 1} & i^+_{L\beta 2} & \dots & i^+_{L\beta n} & i^-_{L\beta 1} & i^-_{L\beta 2} & \dots & i^-_{L\beta n} \end{bmatrix}$$

$$\boldsymbol{i}_{L\gamma} = \begin{bmatrix} i_{L\gamma 1} & i_{L\gamma 2} & \dots & i_{L\gamma n} \end{bmatrix}$$

In addition, if the main voltages are supposed unbalanced and contain harmonics, then they can be expressed with the same way as:

$$\boldsymbol{v}_\alpha = \begin{bmatrix} v^+_{\alpha 1} & v^+_{\alpha 2} & \dots & v^+_{\alpha n} & v^-_{\alpha 1} & v^-_{\alpha 2} & \dots & v^-_{\alpha n} \end{bmatrix}^T$$

$$\boldsymbol{v}_\beta = \begin{bmatrix} v^+_{\beta 1} & v^+_{\beta 2} & \dots & v^+_{\beta n} & v^-_{\beta 1} & v^-_{\beta 2} & \dots & v^-_{\beta n} \end{bmatrix}^T$$

$$\boldsymbol{v}_{L\gamma} = \begin{bmatrix} v_{\gamma 1} & v_{\gamma 2} & \dots & v_{\gamma n} \end{bmatrix}^T$$

Hence, the instantaneous real, imaginary and zero-sequence powers absorbed by the non linear load result from the different interactions between the different harmonics sequences of the load currents and main voltages. In this way, the instantaneous real power components can be expressed in matrix form as follows:

$$\boldsymbol{P}_L = \begin{bmatrix} \boldsymbol{v}_\alpha \\ \boldsymbol{v}_\beta \end{bmatrix} \begin{bmatrix} \boldsymbol{i}_{L\alpha} & \boldsymbol{i}_{L\beta} \end{bmatrix} \tag{8}$$

This matrix contains all possible combinations between positive and negative-sequences of the main voltages and load currents. The diagonal elements are in DC form and all other

elements are in AC form, hence, the DC part of the real power can be expressed as the trace of $\boldsymbol{P}_L$:

$$\bar{p}_L = \sum_{i=1}^{n} (v_{\alpha i}^{+} i_{L\alpha i}^{+} + v_{\alpha i}^{-} i_{L\alpha i}^{-} + v_{\beta i}^{+} i_{L\beta i}^{+} + v_{\beta i}^{-} i_{L\beta i}^{-}) \quad (9)$$

After simplification (9) can be written in $abc-$frames as follows:

$$\bar{p}_L = \bar{p}_{Lf} + \bar{p}_{Lh} \quad (10)$$

Where

$$\begin{aligned} \bar{p}_{Lf} &= 3V_1^{+} I_{L1}^{+} cos(\phi_{V_1^{+}} - \phi_{I_{L1}^{+}}) \\ \bar{p}_{Lh} &= \textstyle\sum_{i=2}^{n} 3V_i^{+} I_{Li}^{+} cos(\phi_{V_i^{+}} - \phi_{I_{Li}^{+}}) \\ &+ \textstyle\sum_{i=1}^{n} 3V_i^{-} I_{Li}^{-} cos(\phi_{V_i^{-}} - \phi_{I_{Li}^{-}}) \end{aligned}$$

V_i^{+}, V_i^{-} and I_i^{+}, I_i^{-} are the rms values of the positive and negative-sequences of the voltage and current components for the i^{th} harmonic, whereas $\phi_{V_i^{+}}$,$\phi_{V_i^{-}}$ and $\phi_{I_{Li}^{+}}$,$\phi_{I_{Li}^{-}}$ are their phase shift respectively.

Equation (10) shows that if the SAPF is controlled to provide constant real power $\bar{p}_L$ drawn from the source, then the source currents remain non sinusoidal because positive and negative sequences of the current that interact with the same sequences at the same frequencies will contribute also to a constant real power exchange $\bar{p}_{Lh}$, consequently, they are not seen as undesirable components, thus non compensated. As a conclusion, to guarantee sinusoidal source current, only $\bar{p}_{Lf}$ must be delivered by the source, in other words, the three-phase source currents must contain only fundamental positive-sequence of the load currents I_{L1}^{+}. However, in the active filter operation, there are some active losses in the power switches and passive filter that cause variations in the DC-bus voltage. To avoid this situation these losses must be compensated by drawing an additional active current I_{loss} from the AC source. This is achieved traditionally by the DC-bus voltage controller that generate the reference signal for I_{loss} from the error between the reference value V_{dc}^{*} and the measured value V_{dc}. Thus the peak source current including the DC-bus voltage regulation is:

$$\hat{I}_s = \hat{I}_{L1}^{+} cos(\phi_{V_1^{+}} - \phi_{I_{L1}^{+}}) + I_{loss} \quad (11)$$

If I_{loss} is generated by a proportional-Integral (PI) controller with k_p and k_i as proportional and integral gains, then:

$$I_{loss} = k_p(V_{dc}^{*} - V_{dc}) + k_i \int (V_{dc}^{*} - V_{dc}) \quad (12)$$

Then, the resulting instantaneous three-phase source current are:

$$\begin{aligned} i'_{sa} &= \hat{I}_s sin(\omega t + \delta_{a1}) \\ i'_{sb} &= \hat{I}_s sin(\omega t + \delta_{b1}) \\ i'_{sc} &= \hat{I}_s sin(\omega t + \delta_{c1}) \end{aligned} \quad (13)$$

Where ω is the fundamental pulsation of the main voltages given by a Phase Locked Loop (PLL), δ_{a1}, δ_{b1} and δ_{c1} are the phase shifts of the fundamental main voltages v_{a1}, v_{b1} and v_{c1} respectively equal to 0, $-\frac{2\pi}{3}$ and $\frac{2\pi}{3}$ if the main voltages are balanced. Theses angles are extracted by a Fourier analysis based detector. In order to compensate the eventual difference ΔV_{dc} between the voltage V_{C1} and V_{C2} across the two capacitors C_1 and C_2 of the DC-bus, the SAPF is forced to absorb a small DC-term current I_{dc} from the AC source such that if the average capacitor voltage V_{C1} is greater than V_{C2}, a negative DC-term current is added to the line current to compensate capacitor C_2. Conversely, if the average capacitor voltage V_{C2} is greater than V_{C1}, a positive DC-term current is added to the line current to compensate capacitor C_1. Hence the instantaneous reference source currents are:

$$\begin{aligned} i_{sa}^{*} &= i'_{sa} + I_{dc} \\ i_{sb}^{*} &= i'_{sb} + I_{dc} \\ i_{sc}^{*} &= i'_{sc} + I_{dc} \end{aligned} \quad (14)$$

The current I_{dc} is computed directly as follows [8]:

$$I_{dc} = K_{dc}(V_{C2} - V_{C1}) \quad (15)$$

To avoid a large DC-term in the source currents, the gain K_{dc} is chosen small and an eventual limiter can be required. Thus, this method proposes a Proportional-Integral+Proportional (PI+P) actions for V_{dc} and ΔV_{dc} control respectively. Finally the compensating currents can be obtained from the reference source current and the load currents as follows:

$$\begin{aligned} i_{ca}^{*} &= i_{sa}^{*} - i_{La} \\ i_{cb}^{*} &= i_{sb}^{*} - i_{Lb} \\ i_{cc}^{*} &= i_{sc}^{*} - i_{Lc} \end{aligned} \quad (16)$$

IV. Sliding Mode Control of the Current Loop

The sliding mode control consists to select the suitable switching configuration of the VSI in order to guarantee the state trajectory attraction toward a predefined sliding surface, and to maintain it stable over this surface. The system established in (7) is a multi-input multi-output non-linear system. In order to formulate the sliding mode creation problem, letting:

$$\boldsymbol{x} = \begin{bmatrix} x_1 & x_2 & x_3 & x_4 & x_5 \end{bmatrix}^T$$

Then (7) can be rearranged in the form [18]:

$$\dot{\boldsymbol{x}} = \boldsymbol{f}(\boldsymbol{x}) + \boldsymbol{G}(\boldsymbol{x})\boldsymbol{u} \quad (17)$$

Where the $(n = 5)$-dimensional vector field $\boldsymbol{f}(\boldsymbol{x})$, the $(n \times m = 5 \times 3)$-dimensional input matrix $\boldsymbol{G}(\boldsymbol{x})$ are given as follows:

$$\boldsymbol{f}(\boldsymbol{x}) = \begin{bmatrix} -\frac{r_c}{L_c}x_1 + \frac{1}{2L_c}x_4 - \frac{1}{2L_c}x_5 - \frac{v_a}{L_c} \\ -\frac{r_c}{L_c}x_2 + \frac{1}{2L_c}x_4 - \frac{1}{2L_c}x_5 - \frac{v_b}{L_c} \\ -\frac{r_c}{L_c}x_3 + \frac{1}{2L_c}x_4 - \frac{1}{2L_c}x_5 - \frac{v_c}{L_c} \\ \frac{1}{2C}x_1 + \frac{1}{2C}x_2 + \frac{1}{2C}x_3 \\ -\frac{1}{2C}x_1 - \frac{1}{2C}x_2 - \frac{1}{2C}x_3 \end{bmatrix}$$

$$\boldsymbol{G}(\boldsymbol{x}) = \begin{bmatrix} \frac{x_4+x_5}{2L_c} & 0 & 0 \\ 0 & \frac{x_4+x_5}{2L_c} & 0 \\ 0 & 0 & \frac{x_4+x_5}{2L_c} \\ \frac{x_1}{2C} & \frac{x_1}{2C} & \frac{x_1}{2C} \\ \frac{x_1}{2C} & \frac{x_1}{2C} & \frac{x_1}{2C} \end{bmatrix}$$

A. Sliding Surfaces

For the n-dimensional controlled system regulated by m independent switches, m sliding surface coordinate functions are defined. To fast track the reference current, let define the three sliding surface coordinate functions in vector form as follows:

$$\boldsymbol{\sigma}(\boldsymbol{x}) = \begin{bmatrix}\sigma_1(\boldsymbol{x})\\ \sigma_2(\boldsymbol{x})\\ \sigma_3(\boldsymbol{x})\end{bmatrix} = \begin{bmatrix}x_1 - x_1^*\\ x_2 - x_2^*\\ x_3 - x_3^*\end{bmatrix} \tag{18}$$

We know yet that when the sliding mode is reached, in other words, when the state vector is forced to evolve on the intersection of the sliding surfaces, i.e. the sliding surface coordinate function $\boldsymbol{\sigma}(\boldsymbol{x})$ must satisfy the following condition: $(\dot{\boldsymbol{\sigma}}(\boldsymbol{x}), \boldsymbol{\sigma}(\boldsymbol{x})) = (\mathbf{0},\mathbf{0})$

Hence, a sliding mode equivalent control denoted by $\boldsymbol{u}_{eq}(\boldsymbol{x})$ may be defined such that the sliding surface coordinate functions $\boldsymbol{\sigma}(\boldsymbol{x})$ satisfy simultaneously the following invariance condition [18]:

$$\dot{\boldsymbol{\sigma}}(\boldsymbol{x}) = \frac{\partial \boldsymbol{\sigma}(\boldsymbol{x})}{\partial(\boldsymbol{x})^T}\Big(\boldsymbol{f}(\boldsymbol{x}) + \boldsymbol{G}(\boldsymbol{x})\boldsymbol{u}_{eq}(\boldsymbol{x})\Big) = 0 \tag{19}$$

We denote $\frac{\partial \boldsymbol{\sigma}(\boldsymbol{x})}{\partial(\boldsymbol{x})^T}\boldsymbol{f}(\boldsymbol{x})$ by $\boldsymbol{L}_f(\boldsymbol{x})$, a m-dimensional vector which represents the directional derivative of $\boldsymbol{\sigma}(\boldsymbol{x})$ along the direction of the vector field $\boldsymbol{f}(\boldsymbol{x})$ as shown in (20). Similarly, the $(m \times m)$-dimensional matrix $\frac{\partial \boldsymbol{\sigma}(\boldsymbol{x})}{\partial(\boldsymbol{x})^T}\boldsymbol{G}(\boldsymbol{x})$ is denoted by $\boldsymbol{L}_G(\boldsymbol{x})$ in (21).

$$\begin{aligned}\boldsymbol{L}_f(\boldsymbol{x}) &= \begin{bmatrix}\frac{\partial\sigma_1(\boldsymbol{x})}{\partial x_1} & \frac{\partial\sigma_1(\boldsymbol{x})}{\partial x_2} & \cdots & \frac{\partial\sigma_1(\boldsymbol{x})}{\partial x_5}\\ \frac{\partial\sigma_2(\boldsymbol{x})}{\partial x_1} & \frac{\partial\sigma_2(\boldsymbol{x})}{\partial x_2} & \cdots & \frac{\partial\sigma_2(\boldsymbol{x})}{\partial x_5}\\ \frac{\partial\sigma_3(\boldsymbol{x})}{\partial x_1} & \frac{\partial\sigma_3(\boldsymbol{x})}{\partial x_2} & \cdots & \frac{\partial\sigma_3(\boldsymbol{x})}{\partial x_5}\end{bmatrix}\boldsymbol{f}(\boldsymbol{x})\\ &= \begin{bmatrix}L_{\boldsymbol{f}1}(\boldsymbol{x})\\ L_{\boldsymbol{f}2}(\boldsymbol{x})\\ L_{\boldsymbol{f}3}(\boldsymbol{x})\end{bmatrix}\end{aligned} \tag{20}$$

$$\begin{aligned}\boldsymbol{L}_G(\boldsymbol{x}) &= \begin{bmatrix}\frac{\partial\sigma_1(\boldsymbol{x})}{\partial x_1} & \frac{\partial\sigma_1(\boldsymbol{x})}{\partial x_2} & \cdots & \frac{\partial\sigma_1(\boldsymbol{x})}{\partial x_5}\\ \frac{\partial\sigma_2(\boldsymbol{x})}{\partial x_1} & \frac{\partial\sigma_2(\boldsymbol{x})}{\partial x_2} & \cdots & \frac{\partial\sigma_2(\boldsymbol{x})}{\partial x_5}\\ \frac{\partial\sigma_3(\boldsymbol{x})}{\partial x_1} & \frac{\partial\sigma_3(\boldsymbol{x})}{\partial x_2} & \cdots & \frac{\partial\sigma_3(\boldsymbol{x})}{\partial x_5}\end{bmatrix}\boldsymbol{G}(\boldsymbol{x})\\ &= \begin{bmatrix}\boldsymbol{L}^l_{\boldsymbol{G}1}(\boldsymbol{x})\\ \boldsymbol{L}^l_{\boldsymbol{G}2}(\boldsymbol{x})\\ \boldsymbol{L}^l_{\boldsymbol{G}3}(\boldsymbol{x})\end{bmatrix}\\ &= \begin{bmatrix}\boldsymbol{L}^c_{\boldsymbol{G}1}(\boldsymbol{x}) & \boldsymbol{L}^c_{\boldsymbol{G}2}(\boldsymbol{x} & \boldsymbol{L}^c_{\boldsymbol{G}3}(\boldsymbol{x})\end{bmatrix}\end{aligned} \tag{21}$$

Where $L_{\boldsymbol{f}j}(\boldsymbol{x})$ $(j = 1,2,3)$ is the j^{th} element in the vector $\boldsymbol{L}_{\boldsymbol{f}}(\boldsymbol{x})$, $\boldsymbol{L}^l_{\boldsymbol{G}j}(\boldsymbol{x})$, $\boldsymbol{L}^c_{\boldsymbol{G}j}(\boldsymbol{x})$ are respectively the j^{th} line and column in the matrix $\boldsymbol{L}_G(\boldsymbol{x})$. Consequently the (19) is rewritten as follows:

$$\dot{\boldsymbol{\sigma}}(\boldsymbol{x}) = \boldsymbol{L}_{\boldsymbol{f}}(\boldsymbol{x}) + \boldsymbol{L}_{\boldsymbol{G}}(\boldsymbol{x})\boldsymbol{u}_{eq}(\boldsymbol{x}) = \mathbf{0} \tag{22}$$

This permits to define the equivalent control in the form:

$$\boldsymbol{u}_{eq}(\boldsymbol{x}) = -\big(\boldsymbol{L}_{\boldsymbol{G}}(\boldsymbol{x})\big)^{-1}\boldsymbol{L}_{\boldsymbol{f}}(\boldsymbol{x}) \tag{23}$$

This means that as a condition for the equivalent control definition is that the matrix $\boldsymbol{L}_{\boldsymbol{G}}(\boldsymbol{x})$must be invertible. Note also that the equivalent control must satisfy $-\mathbf{1} \leq \boldsymbol{u}_{eq}(\boldsymbol{x}) \leq \mathbf{1}$ which the necessary and sufficient condition for the sliding mode existence.

B. Sliding Surface Accessibility

Let consider the following Lyapunov function:

$$V\big(\boldsymbol{\sigma}(\boldsymbol{x})\big) = \frac{1}{2}\boldsymbol{\sigma}^T(\boldsymbol{x})\boldsymbol{\sigma}(\boldsymbol{x}) \tag{24}$$

This positive semi-definite function is identically zero over the surface S, i.e. when $\boldsymbol{\sigma}(\boldsymbol{x}) = \mathbf{0}$ and positive when $\boldsymbol{\sigma}(\boldsymbol{x}) \neq \mathbf{0}$. The quantity $V\big(\boldsymbol{\sigma}(\boldsymbol{x})\big)$ can be interpreted as the distance from the position of the point $\boldsymbol{x}$ in the state space to the desired surface. Therefore, in order to satisfy the condition $\boldsymbol{\sigma}(\boldsymbol{x}) = \mathbf{0}$, the discrete control $\boldsymbol{u} \in \{-1, 1\}^m$ must exercise a closing or opening action, which permits to decrease the distance $V\big(\boldsymbol{\sigma}(\boldsymbol{x})\big)$, this means that the variation of this function in the time must be strictly negative, then;

$$\frac{d}{dt}\Big(V\big(\boldsymbol{\sigma}(\boldsymbol{x})\big)\Big) = \boldsymbol{\sigma}^T(\boldsymbol{x})\dot{\boldsymbol{\sigma}}(\boldsymbol{x}) < 0 \tag{25}$$

This is the condition for the trajectory attraction toward the sliding surface. Referring to (22) and (25), if $\boldsymbol{\sigma}(\boldsymbol{x}) \neq \mathbf{0}$, replacing $\boldsymbol{u}_{eq}(\boldsymbol{x})$ by $\boldsymbol{u}$, then the time derivative of the Lyapunov function can be expressed as follows:

$$\dot{V}\big(\boldsymbol{\sigma}(\boldsymbol{x})\big) = \boldsymbol{\sigma}^T(\boldsymbol{x})\big(\boldsymbol{L}_{\boldsymbol{f}}(\boldsymbol{x}) + \boldsymbol{L}_{\boldsymbol{G}}(\boldsymbol{x})\boldsymbol{u}\big) < 0 \tag{26}$$

Likewise, if $\boldsymbol{\sigma}(\boldsymbol{x}) = \mathbf{0}$, then:

$$\dot{V}\big(\boldsymbol{\sigma}(\boldsymbol{x})\big) = \boldsymbol{\sigma}^T(\boldsymbol{x})\big(\boldsymbol{L}_{\boldsymbol{f}}(\boldsymbol{x}) + \boldsymbol{L}_{\boldsymbol{G}}(\boldsymbol{x})\boldsymbol{u}_{eq}(\boldsymbol{x})\big) = 0 \tag{27}$$

Now, if we consider that the switching frequency is infinite or sufficiently high, we can suppose with good approximation that the state vector $\boldsymbol{x}$ takes the same value in the both cases (26) and (27). Thus, replacing $\boldsymbol{\sigma}^T(\boldsymbol{x})\boldsymbol{L}_{\boldsymbol{f}}(\boldsymbol{x})$ in (26) by its value from (27) the restriction (25) can be reformulated as follows:

$$\dot{V}\big(\boldsymbol{\sigma}(\boldsymbol{x})\big) = \boldsymbol{\sigma}^T(\boldsymbol{x})\boldsymbol{L}_{\boldsymbol{G}}(\boldsymbol{x})\big(\boldsymbol{u} - \boldsymbol{u}_{eq}(\boldsymbol{x})\big) < 0 \tag{28}$$

Hence from (21) the following inequality can be deduced:

$$\sum_{j=1,2,3}\boldsymbol{\sigma}(\boldsymbol{x})^T\boldsymbol{L}^c_{\boldsymbol{G}j}(\boldsymbol{x})u_j < \sum_{j=1,2,3}\boldsymbol{\sigma}(\boldsymbol{x})^T\boldsymbol{L}^c_{\boldsymbol{G}j}(\boldsymbol{x})u_{eqj}(\boldsymbol{x}) \tag{29}$$

Knowing that $-1 \leq u_{eqj}(\boldsymbol{x}) \leq 1$, then (29) can be achieved by applying the following control action:

$$u_j = -sign\Big(\boldsymbol{\sigma}(\boldsymbol{x})^T\boldsymbol{L}^c_{\boldsymbol{G}j}(\boldsymbol{x})\Big) \tag{30}$$

Where $sign$ designs the sign function

C. Switching frequency

The above expressions are rigorously valid only if we suppose that the system is operating with infinite switching frequency. This is an important constraint in practical implementation of the sliding mode control, in fact in such application the switching frequency must be fixed and stabilized at a predefined design value. In order to limit this frequency, a commutation law with fixed hysteresis bandwidth is generally used, therefore. Let suppose that for each restriction $\sigma_j(\boldsymbol{x}) = 0$

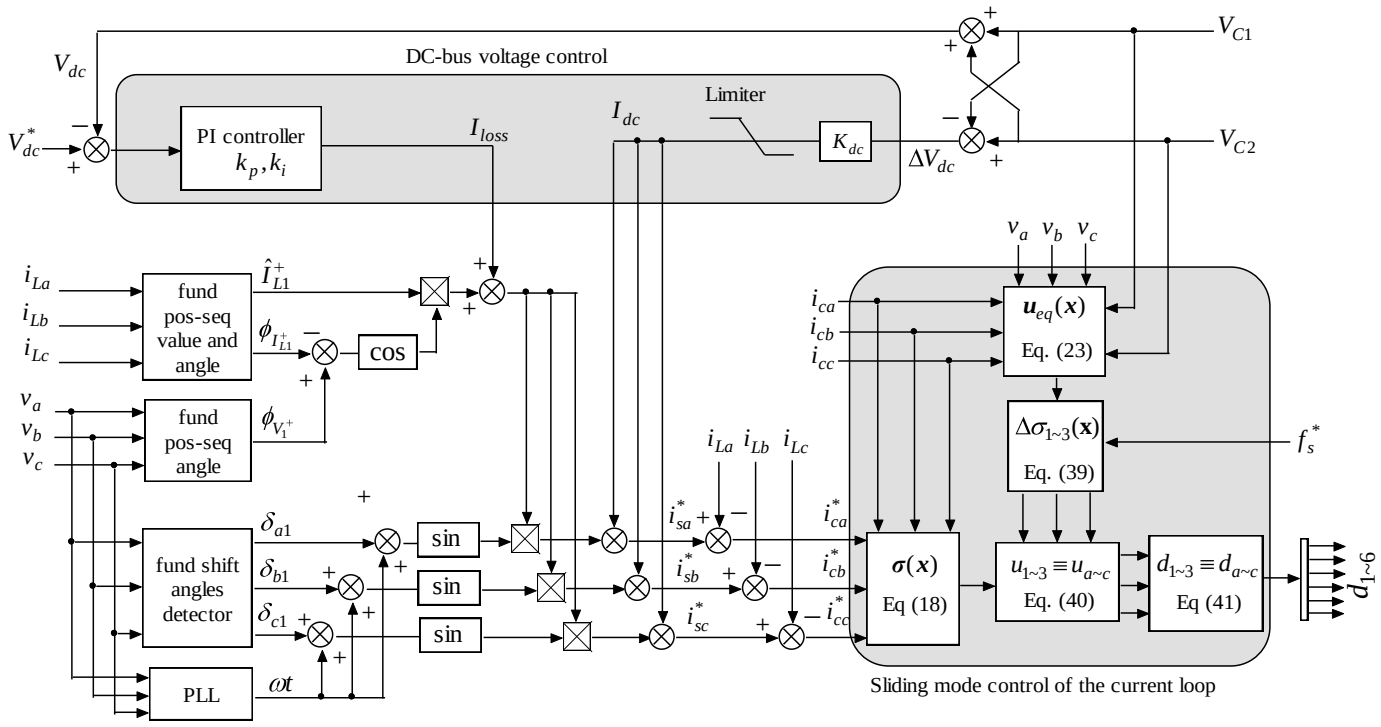

Fig. 2. Complete block diagram of the proposed control.

is assigned a hysteresis band $\Delta\sigma_j(\boldsymbol{x})^*$, therefore $\sigma_j(\boldsymbol{x})$ becomes oscillating between $\pm\Delta\sigma_j(\boldsymbol{x})^*$ and not strictly zero, consequently the control defined in (30) should be redefined as follows:

$$u_j = -sign\Big(\Delta\sigma_j(\boldsymbol{x})^* - \boldsymbol{\sigma}^T(\boldsymbol{x})\boldsymbol{L}^c_{\boldsymbol{G}i}(\boldsymbol{x})\Big) \tag{31}$$

Thus, the time derivative of the j^{th} sliding surface coordinate function is:

$$\begin{aligned}\dot{\sigma_j}(\boldsymbol{x}) = \quad & \boldsymbol{L}_{\boldsymbol{f}j}(\boldsymbol{x}) + \boldsymbol{L}^l_{\boldsymbol{G}j}(\boldsymbol{x})sign\Delta\boldsymbol{\sigma}_j(\boldsymbol{x})^* \\ & -\boldsymbol{L}^l_{\boldsymbol{G}j}(\boldsymbol{x})sign\big(\boldsymbol{\sigma}^T(\boldsymbol{x})\boldsymbol{L}_{\boldsymbol{G}}(\boldsymbol{x})\big)^T\end{aligned} \tag{32}$$

Where $\Delta\boldsymbol{\sigma}(\boldsymbol{x})^* = \Big[\Delta\sigma_1(\boldsymbol{x})^* \quad \Delta\sigma_2(\boldsymbol{x})^* \quad \Delta\sigma_3(\boldsymbol{x})^*\Big]^T$ represents the m hysteresis bandwidths assigned for the m surfaces. If we consider that $\Delta\sigma_j(\boldsymbol{x})^*$ are sufficiently small, therefore, the switching frequency is sufficiently high then we can accept with sufficient approximation that the (32) will be similar to the j^{th} component in (22) which can be written as:

$$\dot{\sigma_j}(\boldsymbol{x}) = \boldsymbol{L}_{\boldsymbol{f}j}(\boldsymbol{x}) + \boldsymbol{L}^l_{\boldsymbol{G}j}(\boldsymbol{x})\boldsymbol{u}_{eq}(\boldsymbol{x}) = 0 \tag{33}$$

This means that $\boldsymbol{L}_{\boldsymbol{f}j}(\boldsymbol{x}) = -\boldsymbol{L}^l_{\boldsymbol{G}j}(\boldsymbol{x})\boldsymbol{u}_{eq}(\boldsymbol{x})$, hence replacing in (32), the following equation can be deduced:

$$\begin{aligned}\dot{\sigma_j}(\boldsymbol{x}) = \quad & \boldsymbol{L}^l_{\boldsymbol{G}j}(\boldsymbol{x})sign\Delta\boldsymbol{\sigma}(\boldsymbol{x})^* \\ & -\boldsymbol{L}^l_{\boldsymbol{G}j}(\boldsymbol{x})sign\big(\boldsymbol{\sigma}^T(\boldsymbol{x})\boldsymbol{L}_{\boldsymbol{G}}(\boldsymbol{x})\big)^T \\ & -\boldsymbol{L}^l_{\boldsymbol{G}j}(\boldsymbol{x})\boldsymbol{u}_{eq}(\boldsymbol{x})\end{aligned} \tag{34}$$

The new control in (31) takes naturally two limit values $\{-1, 1\}$, needed to decrease the difference $|\Delta\sigma_j(\boldsymbol{x})^* - \boldsymbol{\sigma}^T(\boldsymbol{x})\boldsymbol{L}^c_{\boldsymbol{G}j}(\boldsymbol{x})|$ respectively when $\Delta\sigma_j(\boldsymbol{x})^* - \boldsymbol{\sigma}^T(\boldsymbol{x})\boldsymbol{L}^c_{\boldsymbol{G}j}(\boldsymbol{x})$ is positive or negative. Consequently, to respect the stability constraint (26), the (34) is needed to be positive in the switched-on interval t_{on} and negative in the switched-off t_{off} interval respectively. Therefore, these two intervals can be deduced as follows:

$$t_{on} = \frac{2\Delta\sigma_j(\boldsymbol{x})^*}{\dot{\sigma}_j^+(\boldsymbol{x})} = \frac{2\Delta\sigma_j(\boldsymbol{x})^*}{\boldsymbol{L}^l_{\boldsymbol{G}j}(\boldsymbol{x})\big(\mathbf{1} - \boldsymbol{u}_{eq}(\boldsymbol{x})\big)} \tag{35}$$

$$t_{off} = \frac{2\Delta\sigma_j(\boldsymbol{x})^*}{-\dot{\sigma}_j^-(\boldsymbol{x})} = \frac{2\Delta\sigma_j(\boldsymbol{x})^*}{\boldsymbol{L}^l_{\boldsymbol{G}j}(\boldsymbol{x})\big(\mathbf{1} + \boldsymbol{u}_{eq}(\boldsymbol{x})\big)} \tag{36}$$

Where $\dot{\sigma}_j^+(\boldsymbol{x})$ and $\dot{\sigma}_j^-(\boldsymbol{x})$ indicate respectively that the time derivative of $\sigma_j(\boldsymbol{x})$ is positive or negative.
Knowing that the switching frequency is defined as:

$$f_s = \frac{1}{t_{on} + t_{off}} \tag{37}$$

Thus, from (35) and (36), the expression of the switching frequency can be deduced after simplification as follows:

$$f_s = \frac{\Big(\boldsymbol{L}^l_{\boldsymbol{G}j}(\boldsymbol{x})\mathbf{1}\Big)^2 - \Big(\boldsymbol{L}^l_{\boldsymbol{G}j}(\boldsymbol{x})\boldsymbol{u}_{eq}(\boldsymbol{x})\Big)^2}{4\Delta\sigma_j(\boldsymbol{x})^*\boldsymbol{L}^l_{\boldsymbol{G}j}(\boldsymbol{x})\mathbf{1}} \tag{38}$$

The expression (38) shows clearly that the switching frequency f_s depend essentially of the equivalent control vector $\boldsymbol{u}_{eq}(\boldsymbol{x})$ and the predefined hysteresis bandwidth $\Delta\sigma_j(\boldsymbol{x})^*$. If this last one is fixed small, then the switching frequency will be increased, this situation can be recommended for harmonic current control, but in practical applications, this frequency must take a moderate value to limit switching losses and constraints on power switches, especially when the compensated powers are relatively important. Otherwise, the equivalent control is responsible of switching frequency

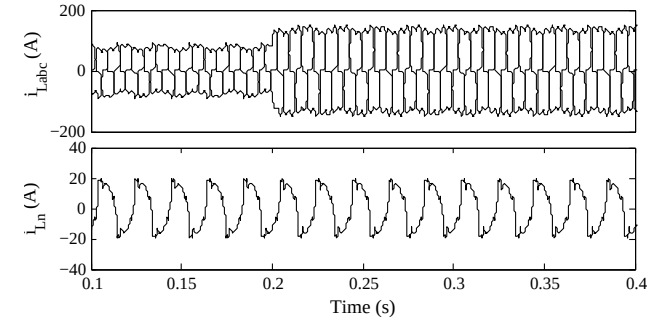

(a) Three-phase and neutral currents without active filtering.

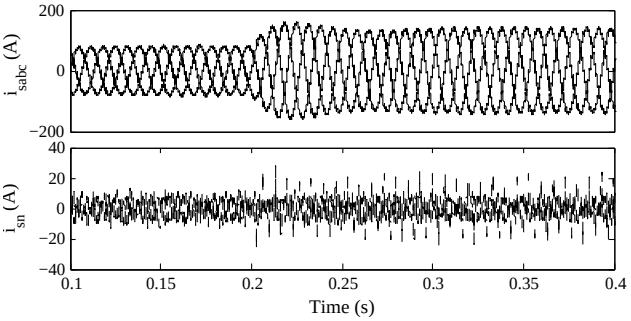

(b) Three-phase and neutral currents with active filtering.

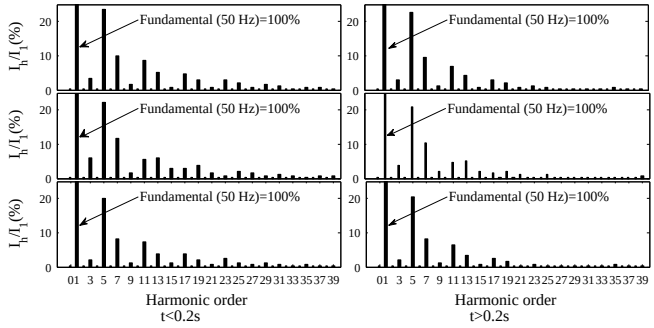

(c) Current spectrums for each phase without active filtering before and after load change.

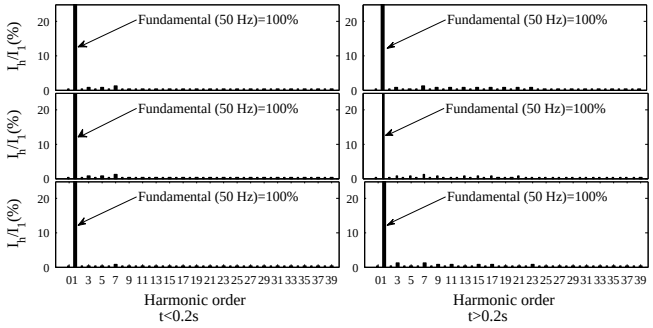

(d) Current spectrums for each phase with active filtering before and after load change.

Fig. 3. Three-phase currents, neutral currents and current spectrums

variations, which can cause audible noise and electromagnetic related problems. In order to solve this problem, in this paper, the hysteresis bandwidth $\Delta\sigma_j(\boldsymbol{x})$ is modulated as a function of the equivalent control $\boldsymbol{u}_{eq}(\boldsymbol{x})$, thus this band will change according to instantaneous value f_s^* of the equivalent control in order to remain the switching frequency nearly constant at a predefined value as it can be seen in the following expression.

$$\Delta\sigma_j(\boldsymbol{x}) = \frac{\Big(\boldsymbol{L}^l_{\boldsymbol{G}j}(\boldsymbol{x})\mathbf{1}\Big)^2 - \Big(\boldsymbol{L}^l_{\boldsymbol{G}j}(\boldsymbol{x})\boldsymbol{u}_{eq}(\boldsymbol{x})\Big)^2}{4f_s^*\boldsymbol{L}^l_{\boldsymbol{G}j}(\boldsymbol{x})\mathbf{1}} \tag{39}$$

And finally the discrete controls u_j and d_j are:

$$u_j = -sign\Big(\Delta\sigma_j(\boldsymbol{x}) - \boldsymbol{\sigma}^T(\boldsymbol{x})\boldsymbol{L}^c_{\boldsymbol{G}j}(\boldsymbol{x})\Big) \tag{40}$$

$$d_j = \frac{1}{2}(1+u_j) \tag{41}$$

The complete block diagram of the proposed control is represented in Fig. 2.

V. Simulation results

The performances of the developed sliding mode control were verified through simulation using MATLAB software. The polluting load is constituted with three-phase thyristor rectifier, single-phase thyristor rectifier and single-phase diode rectifier. For all the simulations, a load variation is operated at $t = 0.2s$. The main parameters of the system are in Table I.

First, in Fig. 3 the three-phase and neutral currents are represented respectively with and without active filtering, with illustrating the harmonic spectrums for each phase. It can be seen from that the current drawn by the load is unbalanced and contains positive-sequence harmonics $6h+5$ (7^{th}, $13^{th}\ldots$), negative-sequence harmonics $6h+5$ (5^{th}, $11^{th}\ldots$), and zero-sequence harmonics $6h+5$ (3^{rd}, $9^{th}\ldots$), where h indicates the harmonic order. Note that the zero-sequence harmonics is the result of the 4^{th}-wire (neutral), this sequence does not appears in the three-wire systems. With the introduction of the active filtering action the three-phase current are sinusoidal and balanced, consequently the current in neutral wire is practically zero. From the Current spectrum in Fig. 3(d), except the fundamental positive sequence, all the undesired harmonics are almost canceled; we can see that the individual harmonic distortions of the other sequence harmonics are all less than 1.2% before and after load change. Table II, detailed THDs and rms values of the currents are summarized.

The above results are obtained under 12.5 KHz as predefined switching frequency. Fig. 4 and Fig. 5 present a comparison between fixed-frequency and free-frequency sliding mode control performances for two predefined values of the switching frequency.

The switching frequencies shown in Fig. 4(a) and Fig. 4(b)

TABLE I
The Main Parameters of the Simulated System.

Phase to neutral voltage source	$230Vrms$, $50Hz$
Source inductance	$L_s = 100\mu H$
DC-bus capacitors	$C_1 = C_2 = 5mF$
DC-bus voltage reference	$V_{dc}^* = 100V$
Inductor filter	$L_c = 2mH$
Switching frequency reference	$f_s^* = 12.5kHz$

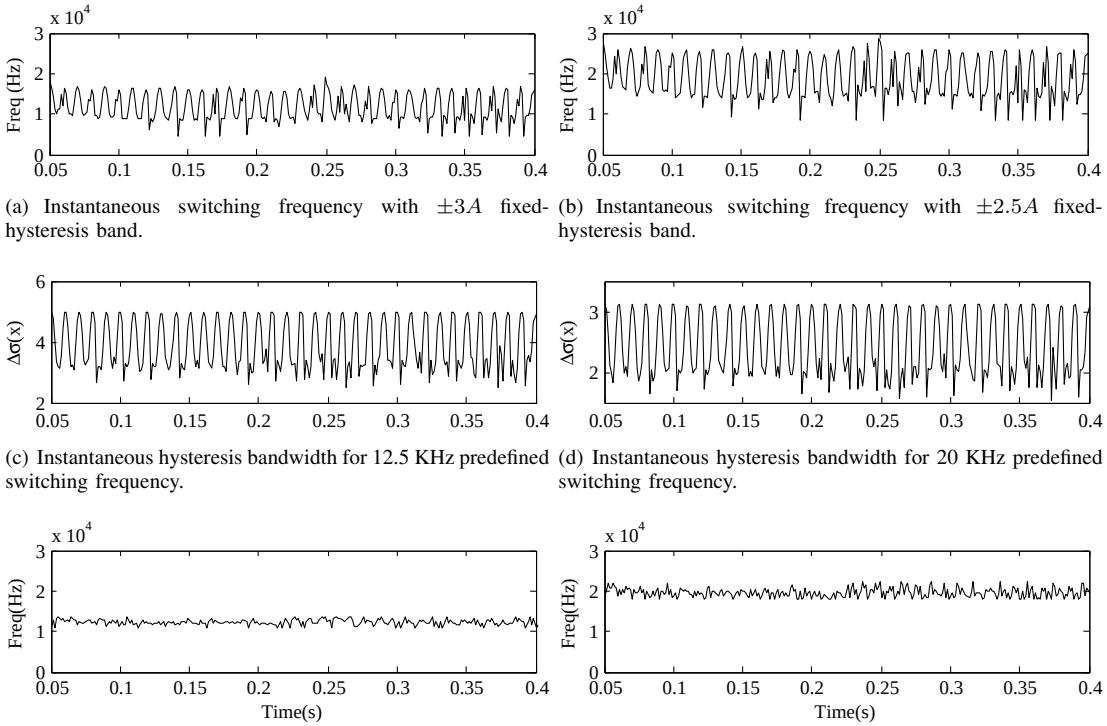

(a) Instantaneous switching frequency with $\pm 3A$ fixed-hysteresis band.

(b) Instantaneous switching frequency with $\pm 2.5A$ fixed-hysteresis band.

(c) Instantaneous hysteresis bandwidth for 12.5 KHz predefined switching frequency.

(d) Instantaneous hysteresis bandwidth for 20 KHz predefined switching frequency.

(e) Instantaneous switching frequency for 12.5 KHz predefined frequency

(f) Instantaneous switching frequency for 20 KHz predefined frequency.

Fig. 4. Switching frequency with free- and fixed-frequency sliding mode control.

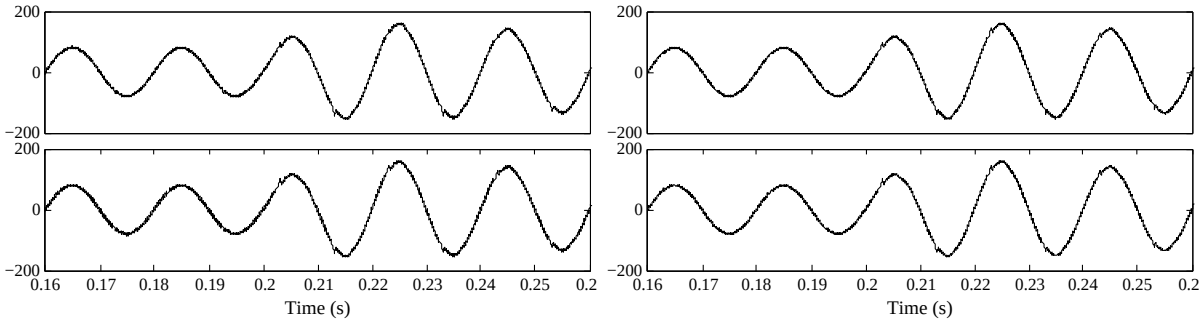

(a) with $\pm 3A$ fixed-hysteresis band (Top) and with 12.5 KHz fixed-frequency control (bottom).

(b) with $\pm 2.5A$ fixed-hysteresis band (Top) and with 20 KHz fixed-frequency control (bottom).

Fig. 5. a-phase wave with free- and fixed-frequency sliding mode control.

TABLE II
DETAILED THDS AND RMS VALUES OF THREE-PHASE AND NEUTRAL CURRENTS BEFORE AND AFTER ACTIVE FILTERING.

3-phase,	$t < 0.2s$		$t < 0.2s$	
Neutral	Before	After	Before	After
THD(%)				
a-phase	28.29	01.70	26.15	02.53
b-phase	27.67	01.48	24.83	02.00
c-phase	23.76	01.76	23.59	02.09
Neutral	31.31	–	31.31	–
RMS				
a-phase	54.03	54.42	98.42	98.00
b-phase	58.74	54.53	105.57	97.51
c-phase	65.21	54.50	108.57	97.58
Neutral	13.10	–	13.10	–

result from a sliding mode control under free-frequency using hysteresis comparators with fixed-bandwidth chosen such that the resulting switching frequencies turn around 12.5 KHz and 20 KHz respectively. In this way the hysteresis bandwidth for the Fig. 4(a) is fixed $\pm 3A$ and $\pm 2.5A$ for the Fig. 4(b). As it can be seen from the two figures, the frequency presents large oscillations (about 60% of the average value). For the

TABLE III
a-PHASE CURRENT THDS WITH FREE-FREQUENCY AND FIXED-FREQUENCY SLIDING MODE CONTROL.

	THD%	
	$t < 0.2s$	$t > 0.2s$
Fixed-bandwidth $\pm 3A$	01.27	02.27
Fixed-frequency 12.5KHz	01.70	02.53
Fixed-bandwidth $\pm 2.5A$	01.23	02.26
Fixed-frequency 20KHz	01.43	02.33

proposed fixed-frequency the instantaneous hysteresis bandwidths computed with respect to the previous frequencies and the instantaneous equivalent control are illustrated respectively in Fig. 4(c) and Fig. 4(d). Remark that these bandwidths are not constant, however the instantaneous switching frequencies resulting from these bandwidths are almost constant as shown in Fig. 4(e) and Fig. 4(f).

Now for the same conditions, the source current in the a-phase is illustrated in Fig. 5 respectively with using free-frequency and fixed-frequency control. The total harmonic distortions are recapitulated in Table III, in this way, it appears that the free-frequency control presents a small superiority in term of current tracking, but no significant difference emerge, in fact the THDs obtained with the two methods are strongly within the standard limits.

VI. Conclusion

In this paper, a sliding mode control under fixed switching frequency of three-phase three-leg voltage source inverter based four-wire shunt active filter using hysteresis comparators to generate the switching signals is achieved. The system is called to compensate distorted and unbalanced currents under non-ideal main voltages. A detailed theoretical analysis of sliding mode and the problematic of the switching frequency limitation is illustrated with simple manner. The adopted solution which consists to use a variable hysteresis band for the switching signals generating has been verified through computer simulation and very satisfactory results have been obtained, in this way, it was verified that the proposed fixed frequency control can conserve the excellent quality of the free frequency control in term of current THD improvement with maintaining the switching frequency nearly constant. As perspectives, the present control seems to be applied successfully to medium or high power electronics converters, like multilevel structures based compensators in power system where a fixed switching frequency is often recommended because of the high power exchange.

References

[1] M. Aredes, J. Häfner, and K. Heulmann, "Three-phase four-wire shunt active filter control strategies," *IEEE Trans. Power. Electron*, vol. 12, no. 02, pp. 311–318, March 1997.

[2] B. Singh, K. Al-Haddad, and A. Chandra, "Harmonic elimination, reactive power compensation and load balancing in three-phase, four-wire electric distribution systems supplying non-linear loads," *Electric Power Syst. Res*, vol. 44, pp. 93–100, 1998.

[3] Singh, K. Al-Haddad, and A. Chandra, "A review of active filters for power quality improvement," *IEEE Trans. Ind. Electron*, vol. 46, no. 5, pp. 960–971, 1999.

[4] Madtharad and S. Premrudeepreechacharn, "Active power filter for three-phase four-wire electric systems using neural networks," *Electric Power Syst. Res*, vol. 60, pp. 177–192, 2002.

[5] A. Cavini, F. Ronchi, and A. Tilli, "Four-wires shunt active filters: optimized design methodology," in *Industrial Electronics Society*. The 29th Annual Conference of the IEEE, 2003, pp. 2288–2293.

[6] B. Lin, H. Chiang, and K. Yang, "Shunt active filter with three-phase four-wire npc inverter," in *IEEE*. The 47th IEEE International Midwest Symposium on Circuits and Systems, 2004, pp. 281–284.

[7] M. Benhabib and S. Saadate, "New control approach for four-wire active power filter based on the use of synchronous reference frame," *Electric Power Syst. Res*, vol. 73, pp. 353–362, 2005.

[8] B. Lin and T. Y. Yang, "Analysis and implementation of three-phase power quality compensator under the balanced and unbalanced load conditions," *Electric Power Systems Research*, vol. 76, pp. 271–282, 2006.

[9] M. Ucar and E. Ozdemir, "Control of a 3-phase 4-leg active power filter under non-ideal mains voltage condition," *Electric Power Syst.*, 2007.

[10] D. Boroyevich, F. C. Lee, R. Zhang, and V. H. Prasad, "Three-dimensional space vector madulatin for four-leg voltage-source conveners," *IEEE trans. power. electronics*, vol. 17, no. 3, 2002.

[11] H. Akagi, Y. Kanazawa, and A. Nabae, "Generalized theory of the instantaneous reactive power in three-phase circuits," in *IPEC'83- Int. Power Elec. Conf*, Tokyo, Japan, 1983, pp. 1375–1386.

[12] V. Siares and P. Verdelho, "Analysis of active power filters in frquency domain using the fast fourier transform," *EPE*, 1997.

[13] H. Bühler, *Réglage par mode de glissement*. Lausane, Suisse: Presse Polytechnique Romandes, 1986.

[14] N. Sabanovic, T. Ninomiya, A. Sabanovic, and B. Perunicic, "Control of three-phase switching converters: A sliding mode approach," PESC 1993.

[15] G. Spiazzi, P. Mattavelli, L. Rossetto, and L. Alesani, "Application of sliding mode control to switch-mode power supplies," *Journal of Circuits, Systems and Computers (JCSC)*, vol. 5, no. 3, pp. 337–354, 1995.

[16] V. Utkin, J. Guldner, and J. Shi, *Sliding Mode Control in Electromechanical Systems*. London: Taylor and Francis, 1999.

[17] M. Ahmed, "Sliding mode control for switched mode power supplies," Ph.D thesis, Lappeenranta University of Technology, Finland, 2004.

[18] H. Sira-Ramirez and R. Silva-Ortigoza, *Control Design Techniques in Power Electronics Devices*. London: Springer-Verlag, 2006.

[19] S.Guffon, A. Toledo, S.Bacha, and G.Bornard, "Indirect sliding mode control of a three-phase active power filter." IEEE, 1998, pp. 1408–1414.

[20] N. Mendalek, K. Al-Haddad, F. Fnaiech, and L. A. Dessaint, "Sliding mode control of 3-phase 3-wire shunt active filter in the dq-frame," CCECE. IEEE, 2001, pp. 765–770.

[21] B. Lin, Z. Hung, S. Tsay, and M. Liao, "Shunt active filter with sliding mode control." IEEE, 2001, pp. 884–889.

[22] B. Bose, "An adaptive hysteresis-band current control technique of a voltage fed pwm inverter for machine drive system," *IEEE Trans. Ind. Electron*, vol. 37, pp. 402–408, 1990.

[23] L. A. Moran, J. W. Dixon, and R. R. Wallace, "A three-phase active power filer operating with fixed switching frequency for reactive power and current harmonic compensation," *IEEE Trans. Ind. Electron*, vol. 42, no. 4, pp. 402–408, 1995.

[24] V. Nguyen and C. Lee, "Tracking control of buck converter using sliding mode with adaptive hysteresis," in *26th Power Electronics Specialists Conference*, Atlanta, USA, 1995, pp. 1086–1093.

[25] J. Zeng, C. Yu, Q. Qi, Z. Yan, Y. Ni, B. Zhang, S. Chen, and F. F. Wu, "A novel hysteresis current control for active power filter with constant frequency," *Electric Power Syst. Res*, vol. 68, pp. 75–82, 2004.

[26] M. Kale and E. Ozdemir, "An adaptive hysteresis band current controller for shunt active power filters," *Electric Power Syst. Res*, vol. 73, pp. 113–119, 2005.

[27] B. Mazari and F. Mekri, "Fuzzy hysteresis control and parameter optimization of a shunt active filter," *Journal of Information Science and Engineering*, vol. 21, pp. 1139–1156, 2005.

[28] M. Navarro-Lopez, D. Cortés, and C. Castro, "Design of practical sliding-mode controllers with constant switching frequency for power converters," *Electric Power Systems Research*, vol. 79, pp. 796–802, 2009.

[29] S. Tan, Y. Lai, and C. Tse, "Implementation of pulse-width-modulation based sliding mode controller for boost converters," *IEEE Power Electron*, vol. 3, no. 4, pp. 130–135, 2006.

[30] S. Buso, L. Malesani, and P. Mattavelli, "Comparison of current control techniques for active filter applications," *IEEE Trans. Power. Electron*, vol. 45, no. 5, pp. 722–729, 1998.